Shape Sensitivity Analysis of Wing Static Aeroelastic Characteristics

Jean-François M. Barthelemy*
NASA Langley Research Center, Hampton, Virginia
and
Fred D. Bergen†
Virginia Polytechnic Institute and State University, Blacksburg, Virginia

A method is presented to calculate the sensitivity derivatives of wing static aeroelastic characteristics with respect to wing shape parameters. The wing aerodynamic response under fixed total load is predicted using Weissinger's L-method; its structural response is obtained with Giles' equivalent plate method. The characteristics of interest in this study include the spanwise distribution of lift, trim angle of attack, rolling and pitching moments, and wing-induced drag, as well as the divergence dynamic pressure. The shape parameters considered are the wing area, aspect ratio, taper ratio, sweep angle, and tip twist angle. Results of sensitivity studies indicate that approximations based on sensitivity derivatives can be used for wide ranges of variations of the shape parameters considered, and the calculation of sensitivity derivatives is significantly less expensive than the conventional finite difference alternative.

Nomenclature

A	= wing aspect ratio
$[A]$	= aerodynamic matrix
a_1,a_2	= chordwise position of the wing-box leading and trailing edges, respectively, normalized by the chord, measured from the leading edge
b	= wing span
$[C]$	= Eq. (9), see details in Ref. 9
$\{cc_l\}$	= vector of product of section lift coefficients and chord length at aerodynamic control stations
$c_{l\alpha}$	= airfoil lift-curve slope
$[D]$	= Eq. (10), see details in Ref. 9
D_i	= wing-induced drag
d	= wing-box depth
E	= modulus of elasticity
$[E]$	= Eq. (11), see details in Ref. 9
e	= position of airfoil center of pressure measured from the quarter-chord point, positive upstream, normalized by the chord
$\{e\}$	= eigenvector, Eq. (12)
$\{e_D^r\},\{e_D^l\}$	= right and left eigenvectors at divergence
$\{f\}$	= vector of applied point loads
G	= shear modulus
$h(x,y)$	= transverse displacement of the wing surface
$[I]$	= identity matrix
$[K]$	= stiffness matrix
L	= lift
M	= flight Mach number
M_r	= rolling moment
N_x,N_y	= order of x and y in the polynominal displacement function $h(x,y)$
n_a	= number of aerodynamic boundary-condition control points along semispan
n_l	= number of applied point loads along semispan
n_s	= number of terms in the approximation to the wing displacement function
p	= generic wing-shape parameters
q	= dynamic pressure
q_D	= divergence dynamic pressure
S	= wing area
$\{s\}$	= vector of amplitudes in the wing transverse displacement function, Eq. (3)
T_r	= pitching moment
t	= wing skin thickness
$\{u\}$	= vector of 1
$[V]$	= diagonal matrix of integration weights
$[W]$	= W_{ij}, value of entry j of vector $\{w\}$ at the point of application of load i
$[W_x]$	= W_{xij}, value of the streamwise derivative of entry j of vector $\{w\}$ at control station i
$\{w(x,y)\}$	= vector of displacement shape functions, Eq. (3)
x	= chordwise coordinate, positive downstream
y	= spanwise coordinate, positive out right wing
α_o	= wing-root angle of attack
$\{\alpha\}$	= vector of angles of attack at aerodynamic control stations
$\{\epsilon\}$	= vector of rigid twist angle
ϵ_t	= wing-tip twist angle, positive nose-up
λ	= taper ratio
Λ	= quarter-chord sweep angle, positive for sweepback
$\{\theta\}$	= vector of elastic twist angle
ν	= Poisson's ratio

Special notations

$\{\ \}$	= column vector
$[\ ]$	= square matrix
$(\ )^t$	= transposed quantity
$[\ ]^{-1}$	= inverse matrix
$(\ )'$	= $\partial(\ )/\partial p$

Received March 3, 1988; presented as Paper 88-2301-CP at the AIAA/ASME/ASCE/AHS 29th Structures, Structural Dynamics and Materials Conference, Williamsburg, VA, April 18–20, 1988; revision received Oct. 30, 1988. This paper is declared a work of the U.S. Government and is not subject to copyright protection in the United States.

*Aerospace Engineer, Interdisciplinary Research Office, Structures Directorate. Member AIAA.
†Graduate Research Assistant. Student Member AIAA.

Introduction

DURING the design phase of an engineering system, numerous analyses are conducted to predict changes in the characterisitcs of the system due to changes in design variables. Usually, this process entails perturbing each variable in turn, recalculating the characteristics, and evaluating the sensitivities using some sort of finite-difference process. The repeated analyses can drive the cost of design very high. Approaches that recently have found increased interest in engineering design are analytical and semi-analytical calculation of the sensitivity derivatives.[1] Typically, these approaches require less computational resource than the finite-difference approach; they are less subject to numerical errors (round-off or truncation). They are best developed in parallel with the baseline analysis capability since they use a significant portion of the numerical information generated for it.

In the design of modern aircraft, airframe flexibility is a concern from strength, control, and performance standpoints. To properly account for the aerodynamic and structural implications of flexibility, reliable aeroelastic sensitivity analysis is needed. Therefore, both structural and aerodynamic sensitivity analysis capabilities are necessary.

Structural sensitivity analysis methodology has been available for well over two decades for both sizing (thickness, cross-section properties) and shape (configuration) variables.[2] However, aerodynamic sensitivity analysis has been nonexistent until relatively recently. Some limited aerodynamic sensitivity analysis capability was developed for aircraft in subcritical compressible flow,[3] but it only handled perturbations in the direction of the thickness of the wing (thickness, camber, or twist distribution). A new approach has been proposed by Yates[4] that considers general geometry variations, including planform for subsonic, sonic, and supersonic-unsteady, nonplanar lifting-surface theory.

Aeroelastic sensitivity analysis methodology has also been available for more than two decades for structural sizing variables (see Ref. 5 for an example application). This is because changes in sizing variables affect exclusively the structural stiffness and mass distribution of the airframe and not its basic geometry. Therefore, structural sensitivity analysis capability is sufficient. However, the lack of development in aerodynamic shape sensitivity analysis explains why aeroelastic shape sensitivity analysis produces very few results.

In a notable exception, Haftka et al.[6] designed a sailplane wing under aeroelastic constraints, and the design model is analyzed with vortex lattice and finite element methods. A finite-difference, aeroelastic sensitivity analysis capability is made possible by 1) devising a reduced order model to describe the wing static aeroelastic response, and 2) using exact perturbation analysis to approximate changes in the vorticity vector with changes in the geometry. Because it retains techniques from both analytical and finite difference sensitivity methodologies, this approach to sensitivity analysis should be described as semi-analytical.

The present study is a proof-of-concept that demonstrates the feasibility of calculating the sensitivity of a wing static aeroelastic characteristics to changes in its shape. Although most of the calculations are analytical, the approach offered here is technically semi-analytical as in Ref. 6, since the stiffness property derivatives are found by finite difference.

Of interest is whether the curvature of the aeroelastic characteristics is small enough to allow use of sensitivity derivatives to approximate them without costly re-analyses. The flight regime is chosen to be subsonic and subcritical so that simple, inexpensive structural and aerodynamic analysis methodologies can be used. Yet the results are felt to be realistic enough that they may be used in conceptual design. It must be noted that the conclusions drawn here are strictly applicable to the analysis methodologies used here and may not hold true for other cases.

This paper first describes the aeroelastic analysis methodology used. It combines Weissinger's L-method[7] to predict the wing spanwise lift distribution with Giles' Equivalent Plate Analaysis[8] method for structural analysis. The calculation of the sensitivity derivatives is described next. Finally, the methodology is used to investigate the sensitivity of a forward swept wing to changes in wing area, aspect ratio, taper ratio, sweep, and tip twist angles. The results are analyzed from the standpoints of both accuracy of extrapolation and computational cost. While the development of the sensitivity equations is given in this paper, the details of the derivation of the coefficients in those equations are given in Ref. 9.

Aeroelastic Analysis

Aerodynamic Model

The wing aerodynamic response is predicted by Weissinger's L-method,[7] which was used herein as implemented for computations by DeYoung and Harpers.[10] It is valid for moderate-to-high-aspect-ratio wings that are symmetric with respect to the root chord, have straight quarter-chord line over each semispan, and have no discontinuities in twist. The airfoil section properties are assumed known and the flight regime may be compressible although it must be subcritical. In this method, the flow around the wing is modeled by a lifting line of vortices bound at the wing quarter-chord line. A no-penetration boundary condition is specified at n_a control stations and determines the spanwise distribution of vortex strength. Weissinger[7] applies the boundary conditions at each station's three-quarter-chord point; DeYoung and Harpers[10] modify that position to account for lift-curve slopes of less than the theoretical 2π and also for effects of compressibility. A linear relationship between the vectors of local angles of attack and lift at the control stations results

$$\{\alpha\} = \frac{1}{2b}[A]\{cc_l\} \tag{1}$$

The aerodynamic matrix $[A]$ depends on the airfoil properties and the Mach number as well as the wing shape. Further details are given in Ref. 9. The total lift developed by the full-span wing is then given by

$$L = \tfrac{1}{2}bq\{u\}^t[V]\{cc_l\} \tag{2}$$

Diagonal $(n_a x n_a)$ matrix $[V]$ contains shape-independent integration weights; its derivation is detailed in Ref. 9.

Structural Model

Giles' Equivalent Plate Analysis method assumes that the wing behaves like a plate and that its transverse displacements can be modeled by a polynomial in the chordwise and spanwise coordinates

$$h(x,y) = \{w(x,y)\}^t\{s\} \tag{3}$$

where $\{w\}$ contains n_s products of various powers of x and y. A careful selection of the exponents of the variables permits the specification of various types of boundary conditions at the wing root. Applying the principle of virtual work, the wing static equilibrium equation under $\{f\}$ of n_l point loads is obtained

$$[K]\{s\} = [W]^t\{f\} \tag{4}$$

$[K]$ is consistent with the displacements given in Eq. (3); it is a function of the wing shape and sizing variables as well as its material properties. This approach has shown very good results for both static and dynamic analysis of wings.[8,11] It can handle fairly general planform geometries and boundary conditions, model complex wing cross-section geometries, include rib and spar caps, and permit the use of composite materials and the consideration of thermal loading.

Aeroelastic Response

To proceed with the calculation of the spanwise distribution of lift and the trim angle of attack under fixed lift, the vector of applied point loads is written in terms of the aerodynamic loads (see Ref. 9):

$$\{f\} = \tfrac{1}{4}bq[V]\{cc_l\} \tag{5}$$

The vector of angles of attack can be written as follows:

$$\{\alpha\} = \alpha_o\{u\} + \{\epsilon\} + \{\theta\} \tag{6}$$

All the entries of $\{u\}$ are 1. Vector $\{\theta\}$ can be derived from Eq. (3). At any control point i, the elastic twist is given by

$$\theta_i = -\frac{\partial}{\partial x} h(x_i, y_i)$$

For consistency with the aerodynamic model, the elastic twist is measured at the three-quarter chord. Then:

$$\{\theta\} = -[W_x]\{s\} \tag{7}$$

Combining Eqs. (1), (4–7), as well as trim Eq. (2), we obtain the unknown angle of attack and the spanwise distribution of lift from:

$$\left\{\begin{bmatrix} [A] + \frac{qb^2}{2}[W_x][K]^{-1}[W]^t[V] & -2b\{u\} \\ \frac{b}{2}\{u\}^t[V] & 0 \end{bmatrix}\right\} \begin{Bmatrix} \{cc_l\} \\ \alpha_o \end{Bmatrix} = \begin{Bmatrix} 2b\{\epsilon\} \\ \frac{L}{q} \end{Bmatrix} \tag{8}$$

Note that the inversion of the stiffness matrix precludes the use of free-body modes. Spanwise integration of the distribution of lift yields the rolling and pitching moments

$$M_r = \frac{qb^2}{8}\{u\}^t[V][C]\{cc_l\} \tag{9}$$

$$T_r = \frac{qb}{4}\{u\}^t[V][D]\{cc_l\} \tag{10}$$

The total induced drag is given in Ref. 9 as:

$$D_i = \frac{\pi q}{8n_a}\{cc_l\}^t[E]\{cc_l\} \tag{11}$$

Matrices $[C]$ and $[E]$ are independent on the wing shape, while matrix $[D]$ is dependent on it. Their derivations are given in Ref. 9.

One can obtain rigid-wing aerodynamic results for the analysis by setting q to zero in the left-hand-side of Eq. (8), and performing the calculations of Eqs. (9–11).

Finally, the wing divergence dynamic pressure is found as the lowest eigenvalue q of the fixed-angle-of-attack problem:

$$\left[[A] + q\left\{\frac{b^2}{2}[W_x][K]^{-1}[W]^t[V]\right\}\right]\{e\} = \{0\} \tag{12}$$

The matrices in Eq. (12) are nonsymmetric; therefore, the system has distinct right and left eigenvectors.

Aeroelastic Sensitivity Analysis

Sensitivity analysis begins with calculation of the derivatives of the distribution of lift and trim angle of attack. Taking the derivative of Eq. (8) with respect to p, we obtain after rearranging:

$$\begin{bmatrix} [A] + \frac{qb^2}{2}[W_x][K]^{-1}[W]^t[V] & -2b\{u\} \\ \frac{b}{2}\{u\}^t[V] & 0 \end{bmatrix} \begin{Bmatrix} \{cc_l\} \\ \alpha_o \end{Bmatrix}'$$

$$= \left\{ \begin{bmatrix} 2(b'\{\epsilon\} + b\{\epsilon\}') \\ 0 \end{bmatrix} - \left\{ \begin{bmatrix} [A]' + \frac{q}{2}[b^2[W_x][K]^{-1}[W]^t]'[V] & -2b'\{u\} \\ \frac{b'}{2}\{u\}^t[V] & 0 \end{bmatrix} \begin{bmatrix} \{cc_l\} \\ \alpha_o \end{bmatrix} \right\} \right\} \tag{13}$$

As for all sensitivity equations, this equation is linear. The coefficient matrix on the left-hand side is identical to that of Eq. (8), which gives the distribution of lift and angle of attack. Furthermore, it does not depend on the parameter with respect to which sensitivity is sought (a similar formulation is used by Yates[4]). Therefore, only one calculation and inversion or factorization of the matrix is necessary for analysis and complete sensitivity analysis. There is one right-hand side vector for each parameter of interest. The derivative of the matrix product $[b^2[W_x][K]^{-1}[W]^t]$ is found by expansion. Calculations for the derivatives of the semispan b and the vector of twist $\{\epsilon\}$, the aerodynamic matrix $[A]$ as well as the matrices $[W_x]$ and $[W]$ are found in Ref. 9. The derivatives of the flexibility matrix ($[K]^{-1}$) are obtained from those of the stiffness matrix. Indeed:

$$[K][K]^{-1} = [I]$$

After taking the derivatives and rearranging:

$$[K]^{-1\prime} = -[K]^{-1}[K]'[K]^{-1} \tag{14}$$

In the present application, even though the sensitivity analysis is performed analytically, the derivatives of the stiffness matrix are found by finite difference. This practice makes the implementation almost as simple as for finite-difference sensitivity analysis, while preserving much of the accuracy and cost advantages of the analytical approach. The shape derivatives of the rolling and pitching moments as well as the wing-induced drag are obtained from Eqs. (9–11). We have:

$$M_r' = \frac{q}{8}\{u\}^t[V]\{2bb'[C]\{cc_l\} + b^2[C]\{cc_l\}'\} \tag{15}$$

$$T_r' = \frac{q}{4}\{u\}^t[V]\{b'[D]\{cc_l\} + b[D]'\{cc_l\} + b[D]\{cc_l\}'\} \tag{16}$$

$$D_i' = \frac{\pi q}{8n_a}(\{cc_l\}'^t[E]\{cc_l\} + \{cc_l\}^t[E]\{cc_l\}') \tag{17}$$

The details of the calculations for matrix $[D]'$ are found in Ref. 9. Rigid-wing results can be obtained if the dynamic pressure is set to zero in Eq. (13).

Table 1 Baseline model parameters

Wing geometry:	
S	$= 20$ m^2
A	$= 7.5$
λ	$= 0.5$
Λ	$= -20$ deg
ϵ_t	$= 0$ deg
Wing structural model:	
a_1	$= 0.2$
a_2	$= 0.7$
t	$= 0.002$ m
d	$= 0.1$ m
Airfoil properties:	
$c_{l\alpha}$	$= 6$
e	$= 0$
Structural properties:	
E	$= 6.89\ 10^7$ kPa
ν	$= 0.3$
G	$= 2.65\ 10^7$ kPa
Loading condition:	
q	$= 4$ kPa
M	$= 0.5$
L	$= 40\ 000$ N
Analytical model discretizations:	
n_a	$= n_l = n_s$
N_x	$= 5$
N_y	$= 6$

The derivatives of the divergence dynamic pressure are found from Eq. (12). If q_D is the divergence dynamic pressure and $\{e_D^r\}$ is the right eigenvector, we have

$$\left[[A] + q_D\left[\frac{b^2}{2}[W_x][K]^{-1}[W]^t[V]\right]\right]\{e_D^r\} = \{0\} \quad (18)$$

Taking the derivative of this expression, pre-multiplying by the transposed left eigenvector $\{e_D^l\}^t$ and rearranging, we find

$$q_D' = \frac{\{e_D^l\}^t\left[[A]' + \frac{q_D}{2}\left[b^2[W_x][K]^{-1}[W]^t\right]'[V]\right]\{e_D^r\}}{\{e_D^l\}^t\left[\frac{b^2}{2}q_D[W_x][K]^{-1}[W]^t[V]\right]\{e_D^r\}} \quad (19)$$

Most of the matrix manipulations required in Eq. (19) have already been performed while calculating the derivatives of lift distribution and angle of attack. Therefore, all that is necessary to evaluate the divergence dynamic pressure derivative is the calculation of the left-hand eigenvector.

Applications

The procedure described here was implemented on a MicroVAX II computer in FORTRAN. Qualitatively, as can be inferred from the derivations, the development and implementation of the sensitivity analysis procedure are little more involved than those of the analysis procedure itself. This section of the paper describes some numerical applications.

The wing model is described by five independent shape parameters: wing area S, aspect ratio A, taper ratio λ, quarter-chord sweep angle Λ, and tip twist angle ϵ_t. The model geometry is depicted in Fig. 1 and the problem parameters are in Table 1.

The derivatives of the stiffness matrix with respect to the shape parameters were found by forward difference. The stepsizes were selected by observing the convergence of various terms in the semi-analytical derivatives of matrix product $b^2[W_x][K]^{-1}[W]^t[V]$; the derivatives were further checked by direct central difference calculations. The following stepsizes were retained: 1% for λ, 0.1% for A, 0.01% for S and Λ.

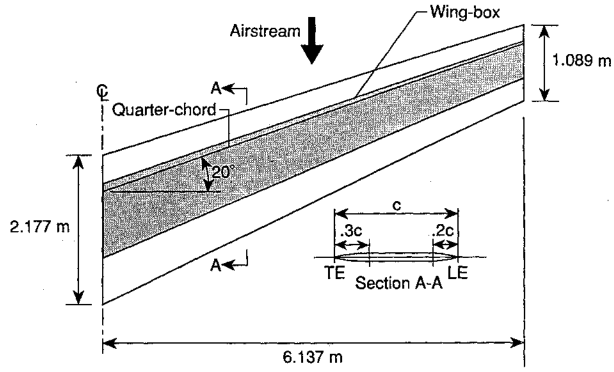

Fig. 1 Baseline wing geometry.

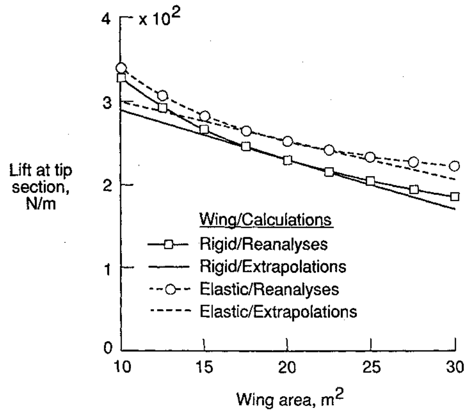

Fig. 2 Sensitivity of lift at wing tip station to wing area.

The number n_a of aerodynamic control stations was varied to examine convergence, and 30 was felt adequate; the effect of varying n_a on accuracy and computational cost will be taken up in a subsequent section of this paper.

The wing structure is an aluminum wing-box of constant depth d and made of two flat cover skins of constant thickness t; it is located between the constant chord locations a_1 and a_2.

A measure of the flexibility of this wing is its divergence dynamic pressure of 16.3 kPa. For an air density of 1 kg/m^3, the airspeed at which the elastic calculations are performed is 89.4 m/s, while the divergence speed is about twice as much at 180.3 m/s.

Results

Sensitivity Results

A sensitivity analysis is performed for the baseline design, and derivatives are generated for rigid-wing and elastic-wing characteristics with respect to the five independent shape parameters. The characteristics include the rigid and elastic spanwise lift distribution (only wing-tip values are given here, since they exhibit maximum aeroelastic effects), trim angle of attack, rolling and pitching moments and induced drag, as well as divergence dynamic pressure. These derivatives are used to approximate changes in the characteristics due to changes in the shape parameters. If $r(p)$ is the value of characteristic r for a value p of a shape parameter, and if $r'(p)$ is the sensitivity derivative of r at p with respect to p, then, for a small Δp, we can write:

$$r(p + \Delta p) \cong r(p) + r'(p)\Delta p \quad (20)$$

In order to gage the quality of the approximations, exact values of the perturbed characteristic $r(p + \Delta p)$ are generated by re-analysis for each value of Δp. Figures 2–7 give examples of the sensitivity results so generated. All the figures share the same layout with the varied independent parameter on the horizontal axis and the characteristic on the vertical axis. Sensitivity results are given for both rigid- and elastic-wing cases.

Table 2 Effect of an aerodynamic model discretization on convergence of elastic induced drag and divergence dynamic pressure and their derivatives

Characteristics and derivatives	$n_a = 10$	$n_a = 30$	$n_a = 50$	$n_a = 70$
D_i^e, N	859.17	852.70	852.19	852.05
$\partial D_i^e/\partial s$, N/m^2	−42.739	−42.300	−42.266	−42.257
$\partial D_i^e/\partial A$, N	−112.72	−111.64	−111.56	−111.53
$\partial D_i^e/\partial \lambda$, N	24.489	27.686	27.936	28.005
$\partial D_i^e/\partial \Lambda$, N/deg	−0.10177	−0.084786	−0.084135	−0.083973
$\partial D_i^e/\partial \epsilon$, N/deg	2.3223	2.8464	2.8850	2.8955
q_D, kPa	16.308	16.254	16.250	16.249
$\partial_D/\partial S$, kPa/m^2	−1.2220	−1.2179	−1.2176	−1.2175
$\partial_D/\partial A$, kPa	−3.8220	−3.8096	−3.8086	−3.8083
$\partial_D/\partial \lambda$, kPa	−8.1577	−8.1288	−8.1265	−8.1259
$\partial_D/\partial \Lambda$, kPa/m^2	6.7952	6.7707	6.7690	6.7685

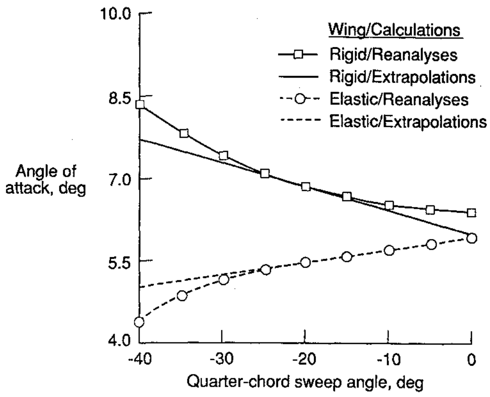

Fig. 3 Sensitivity of trim angle of attack to sweep angle.

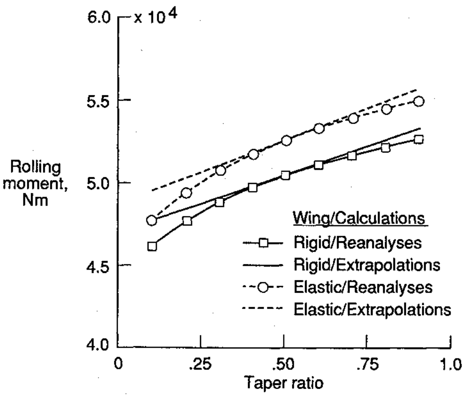

Fig. 4 Sensitivity of rolling moment to taper ratio.

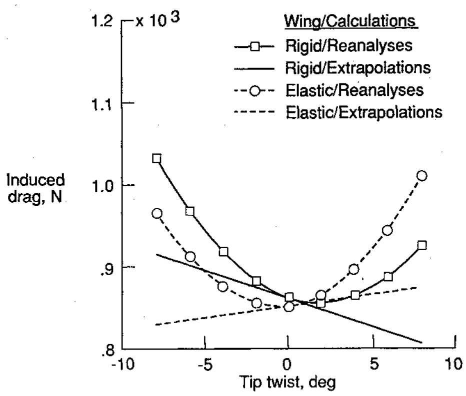

Fig. 5 Sensitivity of induced drag to tip twist angle.

The results display two important properties. First, the straight lines of Eq. (20) are tangent to the corresponding sensitivity curves at the baseline values of the shape parameters, as, of course, they should be. Second, the characteristic's curvatures are small enough so that sensitivity-derivative-based extrapolations can be used to approximate it for a wide range of variation of the shape parameters considered. The range of parameter variations for which the approximations are accurate enough depends largely on the application considered and the stage in the design process. Usually, however, the variations considered in a design effort are significantly smaller than those used in the present calculations, and the quality of the linear approximations should be quite adequate. Indeed, for parameter variations of ± 10% (± 1 deg, for the twist angle), the relative prediction error [|(actual value − predicted value)/actual value|] never exceeds 1% in the results given here. Such a conclusion might differ in flight conditions that involve more complex flows, as in the presence of shock waves or strong viscous interactions.

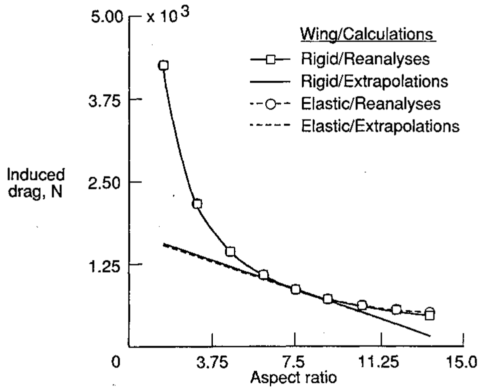

Fig. 6 Sensitivity of induced drag to aspect ratio.

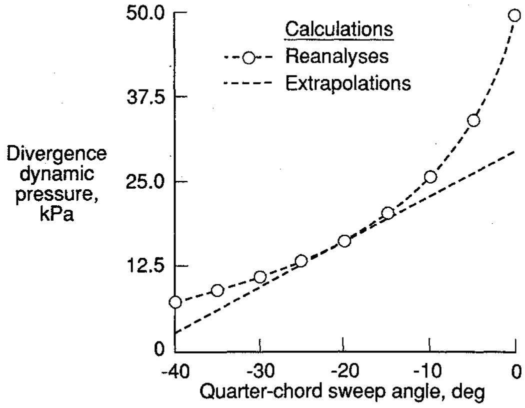

Fig. 7 Sensitivity of divergence dynamic pressure to sweep angle.

Convergence of Calculated Parameters With n_a

The discretization of the aerodynamic model (n_a) is varied to assess its effect on convergence of the parameters and their derivatives. While n_a is varied, the discretization of the structural model is held fixed ($N_x = 5$, $N_y = 6$) because, as indicated in Ref. 8, it cannot be increased significantly without risking singularities in the stiffness matrix.

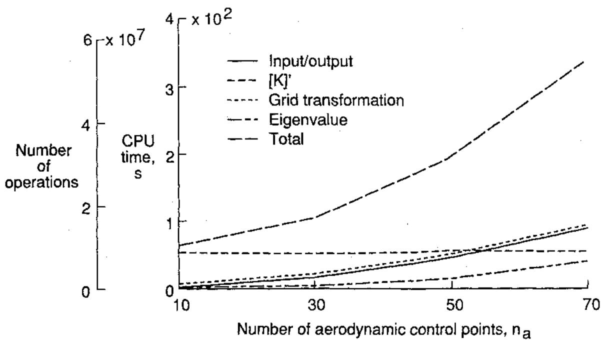

Fig. 8 Cost of finite-difference sensitivity analysis.

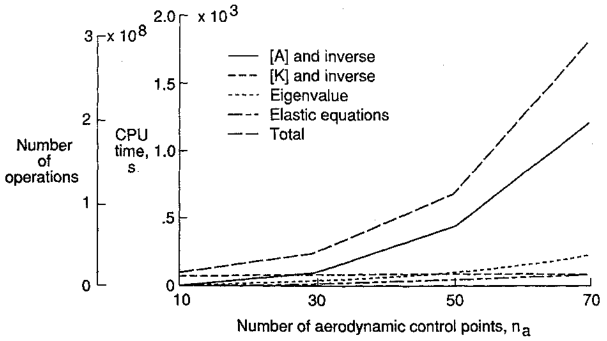

Fig. 9 Cost of semi-analytical sensitivity analysis.

Table 2 shows the effect that aerodynamic discretization has on the convergence of the induced drag and the divergence dynamic pressure, as well as their derivatives. The induced drag and its derivatives converge more slowly than the divergence dynamic pressure. This is probably because the induced drag is very sensitive to variations in the shape of the load distribution and the latter is slow to converge itself. For all the other characteristics considered, the trend is similar to that displayed by the divergence dynamic pressure. Note that, in both cases, the sensitivity derivatives of the characteristics converge about as fast as the characteristics themselves.

Computational Cost

Figures 8 and 9 compare the effect that aerodynamic model discretization has on computational cost and its major components for generation of the sensitivity derivatives by finite difference and semi-analytically. The cost is estimated in terms of both CPU time and total number of floating-point operations. The latter number is based on a double-precision LINPAK computing speed of 0.16 MFLOPS for a MicroVAX II workstation.[12] For finite-difference sensitivity analysis, the cost only includes that of five full re-analyses (one for each independent shape parameter); no effort was made to avoid repeated calculations of invariant quantities. The cost of semi-analytical calculation of the sensitivity derivatives is significantly lower than that of the finite-difference approach; the difference increases as the discretization is refined. For more elaborate analytical procedures that involve two-dimensional (surface panel) or three-dimensional (volume grid) discretizations, this effect is expected to become more pronounced.

For both approaches, the cost associated with the calculations of the stiffness matrix and its derivatives remains constant since the structural model is unchanged. For the finite difference approach, the calculation of the aerodynamic matrix and its derivatives by finite difference is by far the major contributor to the total cost. For the semi-analytical approach, two items dominate the total cost for the finer discretization. First comes the cost of calculating the matrices W and W_x, their derivatives, and the multiplications associated with changes between the discretization of the aerodynamic model and that of the structural model. Second is that of the input/output operations relating to the transfer of information generated during analysis to the sensitivity analysis code. In fact, the cost of computing the derivatives of the aerodynamic matrix is so small that it is not shown on the graph.

Although the cost breakdowns discussed here may not be representative of those obtained with other analysis codes or other computer implementations, these results point to a cost advantage for the semi-analytical approach to sensitivity analysis.

Conclusions

A method is presented to calculate semi-analytically the sensitivity derivatives of wing static aeroelastic characteristics with respect to shape parameters. In this proof-of-concept study, the wing aerodynamic response under fixed total lift is predicted with Weissinger's L-method; its structural response is obtained with Giles' Equivalent Plate Analysis method. Static equilibrium equations are written to determine the spanwise distribution of lift and the trim angle of attack. Spanwise integration of the distribution of lift yields the rolling and pitching moments as well as the induced drag. Finally, the divergence dynamic pressure is obtained as the lowest eigenvalue of the fixed angle of attack problem. Analytical derivatives of the analysis equations yield the sensitivity of the aeroelastic characteristics to changes in the wing area, aspect ratio, taper ratio, quarter-chord sweep angle, and tip twist angle.

The results presented in this study show that, for subsonic-subcritical flow, the curvatures of the wing aeroelastic characteristics are small enough that the characteristics can be well approximated by sensitivity-derivative-based linear extrapolations over ranges of variation of the shape parameters that are wide enough to be useful during the design process. Also, the semi-analytical computation of the sensitivity derivatives is significantly less expensive than the conventional finite-difference approach. In addition, with the simple aerodynamic and structural models used here, the derivation and the implementation of the sensitivity analysis capability are little more complex than those of the corresponding analysis capability.

References

[1]Adelman, H. M., and Haftka, R. T., "Sensitivity Analysis in Engineering," NASA CP 2457, Sept. 1986.

[2]Adelman, H. M. and Haftka, R. T., "Sensitivity Analysis of Discrete Structural Systems," *AIAA Journal,* Vol. 24, May 1986, pp. 823–832.

[3]Hawk, J. D. and Bristow, D. R., "Development of MCAERO Wing Design Panel Method with Interactive Graphics Module," NASA CR 3775, April 1984.

[4]Yates, E. C., Jr., "Aerodynamic Sensitivities from Subsonic, Sonic, and Supersonic Unsteady, Nonplanar Lifting-Surface Theory," NASA TM 100502, Sept. 1987.

[5]Haftka, R. T. and Yates, E. C., Jr., "Repetitive Flutter Calculations in Structural Design," *Journal of Aircraft,* Vol. 13, July 1976, pp. 454–461.

[6]Haftka, R. T., Grossman, B., Eppard, W. M., and Kao, P. J., "Efficient Optimization of Integrated Aerodynamic-Structural Design," Presented at International Conference on Inverse Design Concepts and Optimization in Engineering Sciences-II, University Park, PA, Oct. 1987.

[7]Weissinger, J., "The Lift Distribution of Swept-Back Wings," NACA TM 1120, March 1947.

[8]Giles, G. L., "Equivalent Plate Analysis of Aircraft Wing Box Structures with General Planform Geometry," *Journal of Aircraft,* Vol. 23, Nov. 1986, pp. 859–864.

[9]Barthelemy, J.-F. M. and Bergen, F. D., "Shape Sensitivity Analysis of Wing Static Aeroelastic Characteristics," NASA TP-2808, 1988.

[10]DeYoung, J. and Harpers, C. W., "Theoretical Symmetric Span Loading at Subsonic Speeds for Wings Having Arbitrary Plan Form," NACA Report No. 921, 1948.

[11]Giles, G. L., "Further Generalization of an Equivalent Plate Representation for Aircraft Structural Analysis," NASA TM 89105, Feb. 1987.

[12]Dongarra, J. J., "Performance of Various Computers Using Standard Linear Equations Software in a FORTRAN Environment," Technical Memorandum 23, Argonne National Laboratory, Feb. 1986.